A Numerical Simulation Model of Cable Icing in Freezing Rain Conditions

P. MCCOMBER
Département de Génie Méchanique
École de Technologie Supérieure
Montréal, Québec H2T 2C8, Canada

J. DRUEZ
Université du Québec à Chicoutimi
555, Boulevard de l'Université
Chicoutimi, Québec G7H 2B1, Canada

ABSTRACT

In many countries, the design and reliability of power transmission lines are closely related to atmospheric icing overloads. Thus, accurate ice accretion modeling becomes increasingly important for the optimal design of new lines. At present, most existing icing models assume a uniform circular accretion shape and ice mass along a cable span. But field measurements of ice accretion on cables have shown evidence of variable cable twisting during icing, which can only be modeled by considering an eccentric ice load. By using a more realistic icing shape assumption and considering cable twisting during the simulation, the accuracy of models can be improved.

A model is presented to simulate numerically the wet growth of glaze on a cable of a known torsional compliance. The ice mass and accretion size are calculated on a series of nodes along the cable. First, a heat balance taken on the ice surface yields the icing rate knowing the precipitation rate and incidence direction. Then, at each node, and for each time step, an elliptical ice accretion shape is assumed and the change in eccentricity and orientation is calculated. Finally, from the mass, shape and orientation of the ice accretion, the torque due to gravity and the aerodynamic torsional moment are computed, and the resulting cable twisting is derived for static equilibrium. The aerodynamic moment is approximated by using a semi-empirical expression applicable to a two-dimensional elliptical shape.

An average ice mass load per unit length is finally calculated as a function of time for a cable span. Results verify that twisting of a cable changes the accretion shape and size. Eccentricity of the ice accretion shape is increased for a more rigid cable. Also, the total ice load for a cable span is more important for a smaller cable which is more flexible in torsion.

INTRODUCTION

Atmospheric icing of structures is presently a subject of research interest because of the increasing amount of infrastructures designed for cold regions (Sakamoto, 1990; Makkonen, 1981). An overhead power transmission line is one of the most complicated structures to study, because of its flexibility and movement during icing. Since icing data as well as the meteorological conditions prevailing during an icing storm are difficult to obtain, models have been developed both from icing wind tunnel experiment and by numerical simulation. However, since icing is difficult to reproduce with a reduced scale in a wind tunnel, numerical modeling is being used increasingly (Yip and Mitten, 1991: Makkonen, 1984; McComber, 1984).

Ice accretion samples collected on cables of overhead transmission lines have displayed shapes somewhat different from those obtained on rigid structures. In fact, it has been known for some time that cables twist under the weight of ice (McComber, 1984). Icing has a cumulative effect so that the difference in shape and size influences future accretion. As shown in Fig. 1, rotation can modify the accretion rate on a twisted cable by increasing the effective cross-section. In Fig. 1, the apparent diameter D_f for a fixed cylinder is smaller than D_r the apparent diameter of a twisting cable for rain or D_{rn} the apparent diameter for wind forces.

Traditionally, electric utilities have based their transmission line design on a maximum equivalent radial ice thickness to take into account the icing load. This choice was probably based on observations that ice accretion shapes on a cable are usually fairly circular in shape. Makkonen (1984),

in a previous study, has assumed the ice accretion shape on a cable to be circular, which corresponds to the shape obtained on a rotating cylinder in a wind tunnel. This assumption makes the shape computations, based on one variable only, much simpler. However, using a circular shape makes it impossible to model cable twisting based either on gravity or aerodynamic torques.

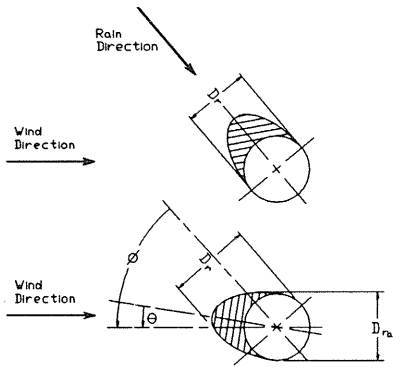

Figure 1 Diagram of ice accretions for fixed and twisted cables, showing the angle of rotation.

On the other hand, in the case of rime icing, McComber (1984) approximated the accretion shape to include cable twisting under the influence of an eccentric ice mass. The approach taken was to consider only the shape in the center of a span and an equivalent span rigidity on both sides.

Gravity is not the only force to consider in the model. McComber et al. (1990a) have suggested that the wind forces will also cause an increased rotation which, in many cases, can be as important as the effects of gravity. Hence, it becomes desirable to include wind forces and the resulting cable rotation in a model for cable icing.

In the following sections, a method to simulate numerically a freezing rain accretion on a cable, while taking into account the twisting of the cable during the accretion, is presented.

GENERAL DESCRIPTION OF THE NUMERICAL SIMULATION MODEL

In order to simulate icing on a cable as a function of time, one has to make an integration of the icing rate with time, as well as an integration along the cable span to obtain the twisting angle.

In order to consider the effect of both gravity and wind force on the accretion, a model predicting the approximate shape along a span is presented. It uses four parameters to describe the shape at each node: two of them to characterize the elliptical shape and two more to locate its center. A finite element approach is taken to determine the twisting angle of each node along the cable span. This model uses two embedded loops, one for the time integration and one for integration along the span. Calculations made in the two loops of the numerical model, i.e. integration in time and space, will be presented in the next two sections.

ICING OF A CABLE ELEMENT

During an icing event, a cable receives a certain amount of supercooled droplets by collision. The liquid water content w is the mass of drops per unit air volume. A portion of drops tends to freeze at impact resulting in an ice accretion. The precipitation intensity, defined as the water impinging on an object, is given by the following expression:

$$I = 3.6\ E\ w\ V_t = 0.001\ \rho_w\ E\ P \qquad (1)$$

where I is the precipitation intensity (kg/m²/h), E the collection efficiency, w the liquid water content (g/m³), V_t the drop vertical or terminal velocity (m/s), P the precipitation rate (mm/h) and ρ_w is the water density (kg/m³).

The collection efficiency, E, is usually calculated for a circular smooth shape using the droplet median volume diameter. However, for rain drops sizes, the collection efficiency is unity. For example, if the precipitation rate is P = 5 mm/h, the droplet median volume diameter will be 1.6 mm (Horjen, 1983). For such a diameter, drops will not be deflected by the air flow near the cable, and the collection efficiency equals unity.

For rain precipitation according to Best (1950), the liquid water content can be related to the precipitation rate by:

$$w = 0.067\ P^{.846} \qquad (2)$$

This estimation of the liquid water content can be used with Eq. (1) to yield the droplet terminal velocity, V_t:

$$V_t = 4.146\ P^{.154} \quad (3)$$

For example, for a precipitation rate of 5 mm/h, the terminal velocity found is $V_t = 5.31$ m/s. The drop velocity V_d and incident angle ϕ can be found from a vector sum of the wind velocity V_a and the terminal velocity Vt.

In the case of wet growth of the accretion, not all of the impinging water freezes. The freezing fraction, f, is defined as the fraction of water impinging on the iced cable that freezes. The freezing fraction can be obtained from a heat balance, developed in a following section, on the surface of the accretion. All the water that remains unfrozen is considered to run off the accretion.

For each time step, the mass accreting is then calculated by:

$$\delta m_i = I \cdot D_r \cdot f \cdot \delta t \quad (4)$$

δm_i is the mass accreted (kg/m), D_r is the cross section normal to the incident rain velocity (m^2/m or m), f the freezing fraction and δt is the time step (h).

The evaluation of the iced cable cross-section, D_r, requires a knowledge of the accretion shape or at least its approximation. If a cylinder is fixed and normal to the droplet flow, an ice accretion approximately elliptical in shape is formed upstream, as shown in Fig. 1. This random shape has to be modeled with sufficient accuracy to determine its influence on the icing rate.

Elliptical shape approximation for icing

Initially, when ice accretion forms on a cylindrical shape, there is a maximum thickness in the direction of the incident rain and a diminishing thickness on each side resulting in an approximately elliptical shape. The icing rate will be at a maximum where the accretion surface is normal to the rain direction and it will decrease as the incidence angle between the rain and the accretion surface decreases. This process tends to create an elongated shape on a more rigid cable, so that it can be modeled by a simple shape, such as an ellipse, with a varying eccentricity adapting to the changing accretion shape.

This can be accomplished by a shape characterized by two parameters to determine the size along the span. This is the minimum number of parameters permitting consideration of a shape with an eccentricity, a first parameter to give the mass or volume of the accretion, and a second one to give the eccentricity of the accretion. But these two parameters could be any other two parameters constraining the geometry. The two parameters chosen in the present model are the major and minor axis, a and b, of the ellipse (see Fig. 2), since they give directly an estimation of the accretion size.

Since it is known that the ice forms mostly on the upstream side of the obstacle, the elongation tends to increase in a nonsymmetrical fashion with respect to the cable center, which will displace the center of gravity of the accretion with respect to the center of rotation. The location of the center of the ellipse with respect to the center of rotation must also be calculated at each time step resulting in two more parameters, r_a and r_b, as shown in Fig. 2.

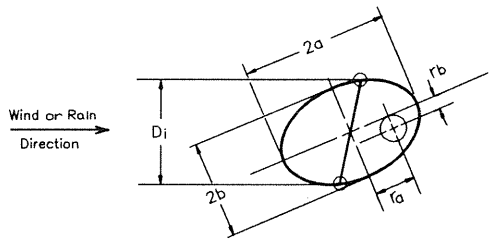

Figure 2 The ellipse with the relative direction of the wind.

Heat balance on the accretion surface

The main contributions in a heat balance equation of a wet icing surface are (Horjen, 1983):

$$Q_c + Q_w + Q_f + Q_o = 0 \quad (5)$$

where Q_c is the heat loss by convection, Q_w is the cooling of the impinging water on the surface, Q_f is the latent heat released during freezing. Q_o the Ohm heating of the conductor must be added to Eq. (6) for live power lines.

In Eq. (5) the heat loss by convection Q_c is:

$$Q_c = A_c\ h\ \delta T \quad (6)$$

where A_c is the heat transfer area m^2, (for an ellipse it is approximated by $Ac = 2\ \pi \sqrt{(a^2 + b^2)/2}$); h is the average heat transfer coefficient ($W/m^2°C$) and δT is the difference between the surface temperature and the

ambient air temperature. As long as a fraction of the impinging water remains in liquid form, the surface temperature is 0°C, the freezing point.

The heat transfer coefficient, h, is not easy to estimate for an ellipse since it varies locally on the cable surface. Here, an average value is used and it is calculated from the heat transfer coefficient of a cylinder with an equivalent diameter corresponding to the section of the iced conductor normal to the wind direction. From the wind velocity, the Reynolds number is calculated ($Re = V_a D_{ra}/\nu$) and the heat transfer coefficient is found from the Reynolds analogy (Rosenhow and Choi, 1961):

$$Pr^{2/3} (h/\rho_a C_p V_a) = 10^x \quad (7)$$
$$where\ x = -1259 - .478(\log(Re) - 2)$$

The heat transfer to the impinging water to the surface in Eq. (5) Q_w is:

$$Q_w = \delta m_i\ Cw\ \delta T \quad (8)$$

The latent heat released during freezing Q_f is:

$$Q_f = f\ \delta m_i\ \lambda \quad (9)$$

where λ (kJ/kg) is the latent heat of fusion of the ice.

Equations (7)-(9) can be combined with Eq. (6) to yield the freezing fraction:

$$f = Ac\ h\ \delta T/\delta m_i\ \lambda + C_w\ \delta T/\lambda - Q_c/\delta m_i\ \lambda \quad (10)$$

New elliptical profile

At each time step, the icing is first calculated from Eq. (4), and then a calculation of the change in major and minor axes of the ellipse, a and b, is performed.

The first part is to calculate the change in the major axis of the ellipse, knowing the ice mass accreting in δt. The angle Θ which is the rotation of the ellipse with respect to the wind direction is also the angle between the wind direction and the normal to the ellipse surface along the major axis. The change, at each time step δt of the major axis, will therefore be:

$$a_{i+1} = a_i + I\ (f\ \delta t/\rho)\ \cos\theta \quad (11)$$

The ice density, ρ (kg/m^3), is used to convert the mass into an accretion volume.

Depending on the rotation angle Θ, the major axis of the ellipse might change and become the second axis b. In such a case, expressions corresponding to Eq. (11) are used for b and δb:

Knowing this change in major axis and the ice mass accreted, m_i, the geometry of the ellipse is found. Since the accretion is mostly on the upstream side and the shape is approximated by a full ellipse, the change in major and minor axes occurs on one side only, and the resulting increases in distance, r_a and r_b, between the center of the ellipse and the center of rotation are:

$$\delta r_a = \delta a/2 \quad ; \quad \delta r_b = \delta b/2 \quad (12)$$

The translation of the center of the ellipse shown in Fig. 2 does not affect the rotational angle Θ, which remains the same for the center of the cable and the center of the elliptical ice shape.

To reduce the possible accumulation of error in the icing rate, that would be the result of the elliptical shape, the ice load obtained from Eq. (4) is used, at each time step, to correct the minor axis of the ellipse, a or b depending on the angle Θ, so that the volume of the accretion corresponds to the volume of the elliptical ice shape.

Cross-section of an ellipse normal to an incident direction

Fig. 3 shows the ellipse centered at the origin with an incident direction making an angle Θ with the x-axis. If (x_i,y_i) are the coordinates of the ellipse on the incident diameter, the two points of the ellipse tangent to the incident direction are located on the conjugate diameter (x_c,y_c). The section of the ellipse normal to the incident direction is found by taking the projection of the conjugate diameter in a direction normal to the incident diameter.

The conjugate diameter coordinates are found from:

$$x_c = a\ \cos(\cos^{-1}(x_i/a) + 90°) \quad (13)$$

$$y_c = b\ \sin(\cos^{-1}(x_i/a) + 90°) \quad (14)$$

Finally, the projection in the direction normal to the incident direction is found from the following scalar product:

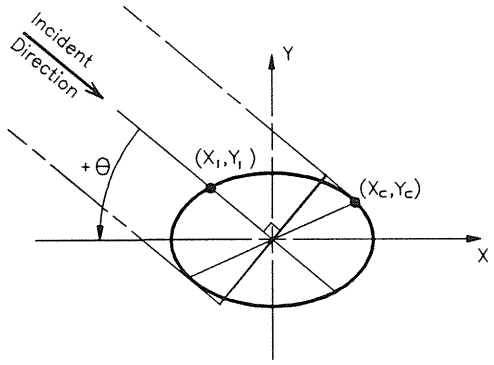

Figure 3 The section of the ellipse perpendicular to the incident direction.

$$D_r = 2\,(x_c \sin|\theta| + y_c \cos|\theta|) \qquad (15)$$

The same formulae Eqs. (13) to (15) are used to find the section perpendicular to the wind direction, D_r, and the rain direction, D_{ra}.

This new value for the cross-section of the ice accretion normal to the wind direction is then used in the next time iteration with Eq. (4).

ROTATION OF THE ICED CABLE

The icing model also requires an integration along the cable span to determine the angle of rotation, Θ, of the ellipse. The cable is divided into n elements. The torsional rigidity of each element is considered constant along the span and is evaluated by:

$$k = GJ/L \qquad (16)$$

where k is the rigidity of an element (N.m/rad), GJ, the rigidity of the cable, the shear modulus, G, multiplied by the polar moment of inertia, J, (m^4) of the section. L is the element length (m). This rigidity is not easily calculated for stranded cables, and measured rigidity in torsion is used in the simulation.

However, since both gravity and aerodynamic torques are dependent on the angle Θ a Newton-Raphson method is used at each time step (McComber and Druez, 1992).

GRAVITY AND AERODYNAMIC TORQUES

The center of gravity of the ice is evaluated, from the distances of the center of the ellipse with respect to the center of rotation:

$$r_{cga} = r_a\,(ab/ab - D^2/4) \qquad (17)$$

$$r_{cgb} = r_b\,(ab/ab - D^2/4) \qquad (18)$$

The gravity torque is found from the ice accretion mass calculated at the center of each element:

$$T_g = m_i\, g\, L\, [r_{cga} \cos\theta + r_{cgb} \sin\theta] \qquad (19)$$

derivative of Eq. (?) with respect to θ is easily found and used in the Newton-Raphson method.

The aerodynamic torque is determined from the torque or moment coefficient by:

$$T_a = (\rho_a\, V_d^2/2)\, D^2\, C_m \qquad (20)$$

The reference diameter, in Eq. (20), is usually taken as the cable diameter.

The aerodynamic torque and the moment coefficient are not easy to determine even for a smooth profile. In the case of growing ice accretion, they can only be approximated.

Potential flow or ideal flow (Milne-Thomson, 1973) around an ellipse at the angle Θ, can be used only as an approximation for high aspect ratio ellipses. Indeed, an elliptical shape is a bluff body and therefore the drag which is not considered in ideal flow plays an important role. The approach taken here is to use the ideal flow theory to estimate the change in the moment coefficent, C_m, with the changing eccentricity of the ellipse. For potential flow the moment coefficient is proportional to c^2, where $c^2 = \sqrt{a^2-b^2}$ and c is the distance of the focus of the ellipse.

$$C_m = (\pi\, c^2/4a^2)\, \sin(2\theta) \qquad (21)$$

where M is the pitching moment per unit length of cable, , and the chord is 2a. The coefficient C_m is therefore proportional to c^2.

However, an empirical value of C_m is used for a reference elliptical size in order to ensure that the order of magnitude of the aerodynamic torque

calculated is realistic. The empirical result obtained for a semi-elliptical shape on a cylinder is used (Richardson, 1980). A small simplification is made to this model. The experiments were conducted on smooth cylinders and there is a measured lift for angle around 180°, which is due to the moving backward of the separation points of the boundary layers for this angle which reduces the form drag. This effect is not included here since in the case of rime, the important roughness of the ice will cause an early separation of the boundary layer, increasing the effect of form drag and decreasing the effect of lift. In view of the moment, coefficient C_m is estimated with the following expressions. For $-45° < 0 < 45°$ $\theta < 45°$, C_m is

$$C_m = 0.32\ c^2 \sin\theta \qquad (22)$$

and for $45° < \theta < 315°$, it is:

$$C_m = 0.32\ c^2\ [1 - (\theta - 45°)/135°] \qquad (23)$$

and the plot of this expression as a function of the angle of attack Θ is given in Fig. 4.

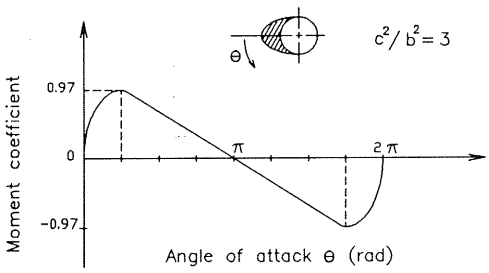

Figure 4 Torque or moment coefficient C_m for an iced cylinder.

The moment coefficient C_m (Eqs. (36)-(37) and Fig. 4) is an approximation and may vary. For example, if the ice profile becomes flatter, then the C_m curve in Fig. 4 will get closer to a sinusoidal curve with its maxima at $\Theta = \pm\pi/2$. But the maximum C_m will still be directly related to the shape eccentricity.

RESULTS OF A COMPUTER SIMULATION CABLE ICING WITH AN ELLIPTICAL SHAPE

The objective of the numerical simulation results presented in this section is to determine the effect of cable twisting on the accretion shape and the icing load in the case of freezing rain.

The parameters chosen for the computer simulation were the following: a precipitation rate of P = 10 mm/h, corresponding to a drop terminal velocity of V_t = 5.31 m/s . The air temperature was chosen to be -2°C; and the accretion density ρ_i was 900 kg/m^3, corresponding to glaze density. The wind velocity was chosen to be V_a = 5 m/s.

Test simulations were done for two cables with characteristics similar to those installed at the experimental icing site of Mount Valin (Canada). One was a larger cable, an ACSR (Aluminium Conductor Steel Reinforced) conductor 0.035 m in diameter and a rigidity of GJ = 351.4 Nm/rad. The second one was a smaller cable, which is used as a ground wire on transmission lines, with D = 0.011 and GJ = 10.8 Nm/rad. The rigidity of the larger cable is based on measurements performed by Hydro-Quebec (McComber, 1984), and the rigidity of the smaller cable is estimated by a comparison of its characteristics with the other cable. The two cables will be referred to as the ACSR conductor (D = 0.035 m) and the ground wire (D = 0.011 m). There is no power on these cables, so that there is no ohm heating (Q_o = 0).

Figure 5 shows a comparison for the ground wire, (D = 0.011 m), of the shape obtained with the model as compared with the shape obtained on a fixed cylinder (k = ∞) and the shape obtained on a rotating cylinder (k = 0). Fig. 5 shows the shape obtained in each case at 0, 25, 50, 75 and 100 min of simulation time. A time step of 5 min was used for the simulation. It can be seen that the fixed cylinder accumulates less ice and the rotating cable more ice. The ice mass accreted on a cable of finite rigidity as calculated by the present model is closer to the results of a rotating cylinder.

Fig 6. shows the increasing mass load m (kg/m), on the ground wire (D = 0.011 m) for the shapes illustrated in Fig. 5. It shows that a fairly compliant cable such as the ground wire collects an amount of ice between the two extreme cases but

closer to the amount collected by a rotating cylinder.

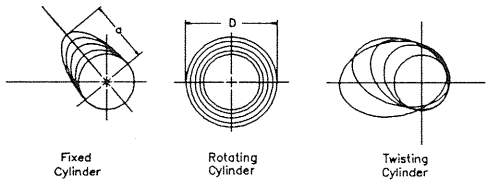

Figure 5 Comparison for the cable (D = 0.011 m) of the shape obtained by the numerical simulation for k = ∞ (fixed), k = 0 (rotating) and k = 10.68 N m/rad. (P = 10 mm/h; T = -2°C, V_a = 5 m/s).

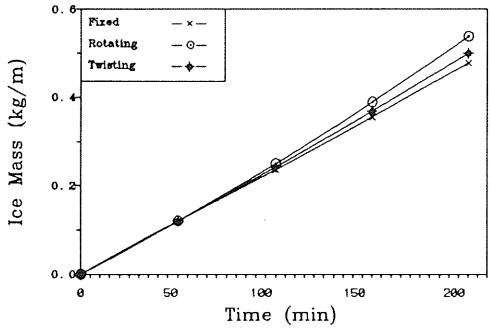

Figure 6 Increasing mass load for fixed, rotating and compliant cable (ACSR conductor, D = 0.035 m). (P = 10 mm/h; T = -2°C, V_a = 5 m/s).

Fig 8. shows the increasing mass load m (kg/m) on the larger ACSR conductor (D = 0.035 m) assuming a rigid cable, the finite rigidity of k = 351.4 N m/rad and finally, a perfectly compliant cable k = ∞. It shows that a more rigid cable gives results closer to those of a fixed cable than those of a rotating cable.

Fig. 9. shows a comparison of the twisted angle during accretion simulated for the ground wire with different wind speeds: 0, 2.5, 5 and 7.5 m/s. Zero angle is the horizontal or wind direction. The case with no wind is equivalent to a calculation with vertical (Θ = -90°) precipitation only. The larger wind velocities decrease the overall rotation angle. This means that in effect the wind moment

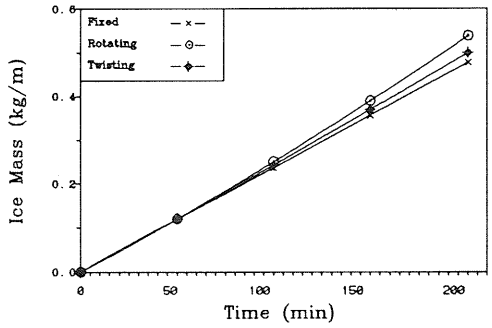

Figure 7 Increasing mass load for fixed, rotating and compliant cable (ACSR conductor, D = 0.035 m). (P = 10 mm/h; T = -2°C, V_a = 5 m/s).

acts in a way as to decrease the apparent compliance of the cable for angle less than 180°. But whereas the gravity effects tends to slow down the rotation at angles of 90° or more, the wind moment is still important at 90° and changes sign only at 180°. However, the aerodynamic force is strongly dependent on the eccentricity of the accretion, so that it has a stronger effect of increasing the rigidity for a cable with larger rigidity as the ACSR conductor. This means that the wind effect increases the difference between a smaller cable and a larger one. Fig. 8 shows that wind forces become significant for wind speeds above V = 7.5 m/s.

Figure 9 shows the increasing mass load as a function of the precipitation rate for the ground wire (ACSR conductor, D = 0.011 m). There is very little difference between precipitation rates of P = 10 and P = 15 mm/h. This confirms that, for wet growth, icing depends more on surface heat transfer than on the amount of impinging drops.

Figure 10 shows the increasing mass load as a function of ambient temperature also for the ground wire (ACSR conductor, D = 0.011 m). There is almost a linear relationship relating the icing rate and the temperature difference between the accretion surface and the ambient temperature.

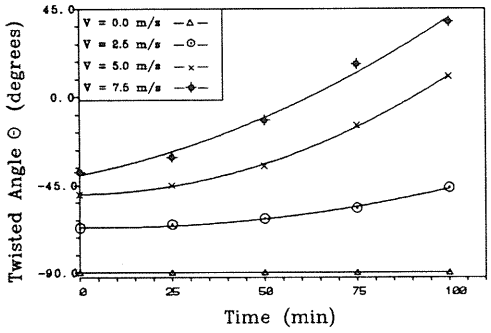

Figure 8 Angle of rotation of the smaller cable (D = 0.11 m) as a function of time for different wind speeds. (P = 10 mm/h; T = -2°C.

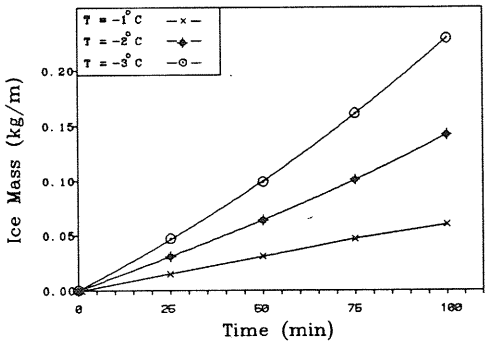

Figure 10 Increasing mass load as a function of ambient temperature (ACSR conductor, D = 0.011 m). (P = 10 mm/h; V = 5 m/s).

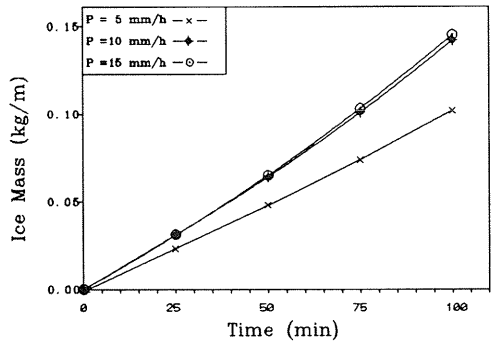

Figure 9 Increasing mass load as a function of the precipitation rate (ACSR conductor, D = 0.011 m). (T = -2°C; V = 5 m/s).

Rotation along a cable span

The curve of the twisted angle Θ along the span is approximately parabolic. This indicates that the maximum strain will occur at the support and the minimum strain in the middle of the span. In such a case, the mechanical breaking of the ice is more likely to occur first at the span extremities.

Comparison of the two cables

Figure 11 compares the relative icing rate of the ground wire and the ACSR conductor. In order to see how one compares with the other the relative mass increase is plotted as a function of time. The relative mass is obtained as the ratio of the total mass to the mass accreted in the first δt (5 min.). This approach was taken because it would take a long time of simulation before the time at which the ground wire would reach the same accretion size as the ACSR cable.

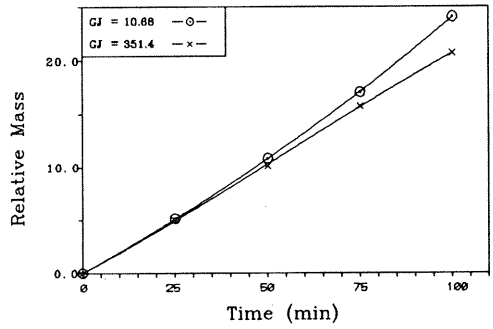

Figure 11 Comparison of the relative icing rates, ground wire (D = 0.0111 m) and ACSR conductor D = (0.035 m), for P = 10 mm/h. (T = -2°C; V = 5 m/s).

Figure 11 shows a relative ice load of 16.2 % more accreted in 100 min. on the smaller cable (D = 0.011 m) when compared with the more rigid cable. The effect for freezing rain is less important

than that obtained for rime icing (McComber and Druez, 1992). This may be due to the fact that for freezing rain, initially gravity and wind torques, because of the incident angle, twist the cable in opposite directions. However, it is difficult to conclude in this case because the wind torque might be smaller or larger than the gravity torque. Even though the simulation was not carried long enough for the accreted load on the small cable to reach the load on the large one, this confirms icing loads measured on these two cables at the Mt. Valin icing site (Druez et al., 1988).

DISCUSSION

The simulation using an elliptical shape model shows that a more compliant cable will have a higher icing rate than a more rigid cable. However, this effect is less pronounced in the case of freezing rain than it is for rime icing (McComber and Druez, 1992). Presently, steel wire having such compliant characteristics are used by electric utilities as ground wires for overhead transmission lines. In such cases, the accretion rate of the smaller cable could be reduced by fixing weight pendulums along the span. These pendulums, by making the cable more rigid in torsion, would reduce potential ice accretion loads and therefore hopefully would reduce damages due to atmospheric icing.

The elliptical model presented here is certainly more complicated than a circular model since it must compute at each time step four parameters, a, b, r_a and r_b at different locations on a cable span. However, it is a model which can predict, as observed during field measurements (Druez et al., 1988), a larger accretion on a smaller cable, and also can include aerodynamic forces into the simulation. The aerodynamic forces are responsible for the mechanical breaking of the ice and shedding during an icing event and therefore are important for a complete and reasonably accurate accretion model.

The present model is a compromise between the oversimplified circular shape and the exact icing shape at each time step. Even though modern computers offer much cheaper computation time, it seems that an accurate simulation of the changing accretion shape, even in the case when a finite element approximation is used (McComber, 1984), will result in a model too complicated and difficult to verify. The accuracy needed to describe the icing shape should be related to the sensitivity of the shape in the computation of the overall icing load. For example, in order to reduce computation time, the time step δt can be chosen large enough to correspond to a significant rotation angle at each step.

By including the effect of the wind in the calculation, more realistic shapes can be obtained. However, only the average wind velocity was used in the simulation. The effect of a fluctuating wind velocity would be a corresponding change in the cable twisting angle Θ. This would have the effect of creating a more circular shape.

An advantage of having the aerodynamic forces calculated is that it makes it possible to determine the stresses occurring in the ice accretion. Calculation of the maximum stresses can be done easily on a simple shape such as an ellipse, McComber et al. (1990a) have suggested that these stresses occur at both ends of a span at the supports and are probably responsible for mechanical breaking of ice chunks. The calculation of this stress can eventually permit the inclusion in the model of a shedding rate which was shown to be correlated to the wind speed squared (McComber et al., 1990b).

However, the aerodynamic force, probably as important as gravity for speeds of about 7.5 m/s, is not easy to estimate. An approximation for an elliptical shape, based on experimental values obtained in wind tunnel for similar shapes, is used in the present model. This gives a rough estimate of the order of magnitude of the force and its effect.

With the development of meteorological instruments permitting measurements of the icing rate at various sites as well as the standard meteorological parameters, it is hoped that this numerical simulation model will be useful in calculating the predicted loads on overhead power transmission lines.

CONCLUSIONS

The twisting of cables during atmospheric icing is an important factor to consider in the numerical simulation of cable icing. Indeed, it can explain the differences in ice accretions heads obtained on smaller and more compliant cables. It is possible to

model this characteristic through the use of an elliptical approximation of the shape, instead of the traditional circular shape approximation.

For cables with lower torsional rigidity, the shape obtained by a freezing rain simulation is more circular and the center of gravity becomes closer to the vertical line, both effects resulting in a lower twisting moment developed by the accretion weight and wind force. For a more rigid cable, the accretion shape becomes more eccentric and results in less rotation. The simulation for an ACSR conductor shows that the growth of the accretion is not as fast for a more rigid cable of this type. This effect is less pronounced in the case of freezing rain than for rime accretion.

When the aerodynamic force is added to the gravity force, it tends to modify the effective torsional rigidity of the cable. In so doing, an increase in accretion rate is obtained. It is essential to account for the combined action of the wind. It increases the precipitation intensity and also icing by increasing the surface heat transfer. It modifies the effective torsional rigidity of the cable; and finally, it creates a wind load to be considered in the overall load due to icing on transmission lines.

ACKNOWLEDGEMENTS

This work was supported by the Natural Sciences and Engineering Research Council of Canada (NSERC) and the Fonds de Développement Académique du Réseau (FODAR) of the Université du Québec.

REFERENCES

Best, A.C., (1950). "The Size Distribution of Raindrops", Quart. J. Roy. Met. Soc., Vol 76, pp. 16-36.

Druez, J., McComber, P., Félin, B., (1988). "Icing Measurements Made for Different Cable Configurations on an Icing Test Line at Mt. Valin", Proc. Fourth Int. Workshop on Atmospheric Icing of Structures, Paris, pp. 124-128.

Horjen, I., (1983). "Icing of Offshore Structures-Atmospheric Icing" Norwegian Marime Research, No 3, pp. 9-22.

Makkonen, L., (1981). "Estimating intensity of atmospheric ice accretion on stationary structures.", J Appl. Meteorol., Vol 20, No 5, pp. 595-600.

Makkonen, L., (1984). "Modeling of Ice Accretion on Wires ", J. of Applied Meteor. Vol 23, pp. 929-939.

McComber, P., (1984). "Numerical simulation of Cable Twisting Due to Icing", Cold Regions Science and Technology, Vol 8, pp. 253-259.

McComber, P., Druez, (1992). "A Numerical Simulation Model of Cable Icing Using an Elliptical Ice Shape", Proceedings of the Second (1992) Int. Offshore and Polar Eng. Conf. ISOPE 1992, Vol. II, San Francisco, June 15-19, 1992, pp. 632-640.

McComber, P., Druez, J., St-Louis, M., (1990a). "Effects of Twisting Motion on Atmospheric Ice Shedding", Fifth International Workshop of Atmospheric Icing of Structures, Tokyo, October 1990.

McComber, P. Druez, J., Félin, B., (1990b). "Cable Rime Accretion on a Laurentian Mountain", Rev. can. de génie civil, Vol 17, pp. 1022-1032.

Milne-Thomson, L.M., (1973). "Theoretical Aerodynamics", Fourth Edition, Dover Publications, New-York, 430 p.

Richardson, A.S., (1980), "Some Effect of Conductor Twisting on Galloping", IEEE Trans. Power App. and Systems, Vol PAS-99, No 2, pp. 811-822.

Rohsenow, W.M., Choi, H., (1961). "Heat, Mass and Momentum Transfer", Prentice Hall, Englewood Cliffs, N.J., 537 p.

Sakamoto, Y., (1990). "Ice and Snow Accretion on Structures in Japan", Fifth International Workshop of Atmospheric Icing of Structures, Tokyo, October 1990.

Yip, T.C., Mitten, P., (1991). "Comparison Between Different Ice Accretion Models", Canadian Electrical Association Centennial Conference, Toronto, May 1991.